

Turbulent Thermal Diffusion in a Multi-Fan Turbulence Generator with the Imposed Mean Temperature Gradient

A. Eidelman, T. Elperin,* N. Kleeorin, I. Rogachevskii, and I. Sapir-Katiraie

The Pearlstone Center for Aeronautical Engineering Studies, Department of Mechanical Engineering, Ben-Gurion University of the Negev, Beer-Sheva 84105, P. O. Box 653, Israel

(Dated: September 30, 2018)

We studied experimentally the effect of turbulent thermal diffusion in a multi-fan turbulence generator which produces a nearly homogeneous and isotropic flow with a small mean velocity. Using Particle Image Velocimetry and Image Processing techniques we showed that in a turbulent flow with an imposed mean vertical temperature gradient (stably stratified flow) particles accumulate in the regions with the mean temperature minimum. These experiments detected the effect of turbulent thermal diffusion in a multi-fan turbulence generator for relatively high Reynolds numbers. The experimental results are in compliance with the results of the previous experimental studies of turbulent thermal diffusion in oscillating grids turbulence (Buchholz et al. 2004; Eidelman et al. 2004). We demonstrated that turbulent thermal diffusion is an universal phenomenon. It occurs independently of the method of turbulence generation, and the qualitative behavior of particle spatial distribution in these very different turbulent flows is similar. Competition between turbulent fluxes caused by turbulent thermal diffusion and turbulent diffusion determines the formation of particle inhomogeneities.

PACS numbers:

I. INTRODUCTION

The main goal of this study is to describe the experimental investigation of the effect of turbulent thermal diffusion in a multi-fan turbulence generator. Turbulent thermal diffusion is associated with the correlation between temperature and velocity fluctuations in a turbulent flow with an imposed mean temperature gradient and causes a relatively strong non-diffusive mean flux of particles in the direction of the mean heat flux. This effect results in the formation of large-scale inhomogeneities in particle spatial distribution whereby particles accumulate in the vicinity of the minimum of the mean fluid temperature. Turbulent thermal diffusion was predicted theoretically by Elperin et al. (1996; 1997) and detected experimentally by Buchholz et al. (2004) and Eidelman et al. (2004) in oscillating grids turbulence.

The mechanism of the phenomenon of turbulent thermal diffusion for inertial solid particles is as follows. Inertia causes particles inside the turbulent eddies to drift out to the boundary regions between the eddies (i.e., regions with low vorticity and maximum of fluid pressure). Therefore, particles accumulate in regions with maximum pressure of the turbulent fluid. Similarly, there is an outflow of particles from regions with minimum pressure of fluid. In a homogeneous and isotropic turbulence without large-scale external gradients of temperature, a drift from regions with increased or decreased concentration of particles by a turbulent flow of fluid is equiprobable in all directions, as well as pressure and temperature of the surrounding fluid do not correlate with the tur-

bulent velocity field. Therefore, only turbulent diffusion determines the turbulent flux of particles.

In a turbulent fluid flow with a mean temperature gradient, the mean heat flux is not zero, i.e., the fluctuations of temperature and the velocity of the fluid are correlated. Fluctuations of temperature cause fluctuations of fluid pressure. These fluctuations result in fluctuations of the number density of particles. Indeed, an increase of pressure of the surrounding fluid is accompanied by an accumulation of particles due to their inertia. Therefore, the direction of the mean flux of particles coincides with that of the heat flux, and the mean flux of particles is directed to the region with minimum mean temperature, and the particles accumulate in this region (Elperin et al. 1996).

The mechanism of turbulent thermal diffusion is associated with a nonzero divergence of a particle velocity field. The latter is caused either by particle inertia or inhomogeneity of fluid density in a non-isothermal low-Mach number turbulent fluid flow. Therefore, the effect of turbulent thermal diffusion can be also observed in the suspension of non-inertial particles (e.g., particles with a Stokes time of the order of $10^{-6} - 10^{-5}$ s in air flows) or for gaseous admixtures in non-isothermal low-Mach number turbulent fluid flows (see Elperin et al., 1997). Note that when we refer to compressible non-isothermal fluid flow with low Mach numbers, it means that $\text{div}(\rho \mathbf{v}) \approx 0$, where \mathbf{v} is the fluid velocity and ρ is the fluid density. The latter implies that $\text{div} \mathbf{v} \approx -(\mathbf{v} \cdot \nabla)\rho/\rho \neq 0$. In particular, in a non-isothermal fluid flow with a temperature gradient $\text{div} \mathbf{v} \approx -(\mathbf{v} \cdot \nabla)\rho/\rho \approx (\mathbf{v} \cdot \nabla)T/T \neq 0$, where T is the fluid temperature.

Numerical simulations, laboratory experiments and observations in the atmospheric turbulence revealed formation of long-living inhomogeneities in spatial distri-

*Electronic address: elperin@bgu.ac.il

bution of small inertial particles and droplets in turbulent fluid flows (see, e.g., Wang and Maxey 1993; Korolev and Mazin 1993; Eaton and Fessler 1994; Fessler et al. 1994; Maxey et al. 1996; Aliseda et al. 2002; Shaw 2003). The origin of these inhomogeneities was intensively studied by Elperin et al. (1996; 1997; 2000a; 2000b). It was pointed out that the effect of turbulent thermal diffusion is important for understanding different atmospheric phenomena (e.g., atmospheric aerosols, smog formation, etc). In particular, the existence of a correlation between the appearance of temperature inversions and the aerosol layers (pollutants) in the vicinity of the temperature inversions is well known (see, e.g., Csanady 1980; Seinfeld 1986; Flagan and Seinfeld 1988). Turbulent thermal diffusion can cause the formation of large-scale aerosol layers in the vicinity of temperature inversions in atmospheric turbulence (Elperin et al. 2000a; 2000b). Observations of the vertical distributions of pollutants in the atmosphere show that maximum concentrations can occur within temperature inversion layers (see, e. g., Csanady 1980; Seinfeld 1986; Jaenicke 1987). The characteristic parameters of the atmospheric turbulent boundary layer are: the maximum scale of turbulent flow is $L \sim 10^3 - 10^4$ cm; the turbulent fluid velocity in the scale L is $u \sim 30 - 100$ cm/s; the Reynolds number is $Re = uL/\nu \sim 10^6 - 10^7$ (see, e. g., Csanady 1980; Seinfeld 1986; Blackadar 1997), where ν is the kinematic viscosity. For instance, for particles with material density $\rho_p \sim 1 - 2$ g / cm³ and radius $a = 20$ μ m the characteristic time of formation of inhomogeneities is of the order of 1 hour for the temperature gradient 1K/100 m and 2 hours for the temperature gradient 1K/200 m. The effect of turbulent thermal diffusion might be also of relevance in different industrial non-isothermal turbulent flows (Elperin et al. 1998).

Turbulent thermal diffusion is a new and fundamental phenomenon. Therefore, this phenomenon should be studied for different types of turbulence and different experimental set-ups. Previously phenomenon of turbulent thermal diffusion was studied experimentally only in oscillating grids turbulence whereby the Reynolds numbers were not so high (see for details Buchholz et al. 2004; Eidelman et al. 2004). In order to study the effect of turbulent thermal diffusion at higher Reynolds numbers we constructed a multi-fan turbulence generator. Similar apparatus was used in the past in turbulent combustion studies (Birouk et al. 1996) and in studies of turbulence-induced preferential concentration of solid particles in microgravity conditions (Fallon and Rogers 2002). The multi-fan turbulence generator allows us to produce nearly homogeneous isotropic turbulent fluid flow with a small mean velocity. Using Particle Image Velocimetry and Image Processing Techniques we determined velocities and spatial distribution of tracer particles in the isothermal and non-isothermal turbulent flows. Our experiments with non-isothermal turbulent flows were performed for a stably stratified fluid flow with a vertical mean temperature gradient which was formed

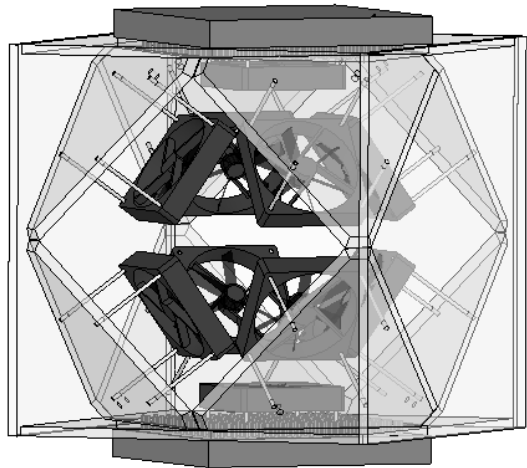


FIG. 1: The scheme of the test section.

by a cooled bottom wall and a heated top wall of the chamber. We found that particles accumulate in the vicinity of the bottom wall of the chamber (where the mean fluid temperature is minimum) due to the effect of turbulent thermal diffusion. Sedimentation of particles in a gravity field in these experiments was very slow in comparison with accumulation of particles caused by turbulent thermal diffusion. In the present study we demonstrated that turbulent thermal diffusion occurs independently of the method of turbulence generation.

II. EXPERIMENTAL SET-UP

A multi-fan turbulence generator includes eight fans (120 mm in outer diameter and with controlled rotation frequency of up to 2800 rpm) mounted in the corners of a cubic Perspex box and facing the center of the box. The Perspex box is a cube $400 \times 400 \times 400$ mm³, with eight 272 mm equilateral triangles mounted in its corners used as solid bases for the fans (see Fig. 1). Each fan was calibrated separately, and the input current and rotation speed were measured and logged. We also tested one fan operating above an electric heat source. We placed a thermocouple in the vicinity of the fan's motor, and repeated this test for different temperatures (290, 310, 330 K). These experiments showed that the fan rotation speed does not depend on the temperature.

At the top and bottom walls of the Perspex box we installed two heat exchangers with rectangular $3 \times 3 \times 15$ mm³ fins. The upper wall was heated up to 343 K, the bottom wall was cooled to 283 K. Therefore, comparatively large vertical mean temperature gradient (~ 92 K/m) was formed in the core of the flow. The temperature was measured with a high-frequency response thermocouple (0.005 inches in diameter) which was glued externally to a wire (2.2 mm of Cu in diameter coated with 0.85 mm Teflon). The accuracy of the temperature

measurements was of the order of 0.1 K. We found that the temperature measurements affected the flow in a very small area around the wire. Two additional fans were installed at the bottom and top walls of the chamber in order to produce a large mean temperature gradient in the core of the flow. Our measurements showed that these two additional fans only weakly affected considerably the homogeneity and isotropy of the turbulent flow.

Velocity fields were measured using Particle Image Velocimetry (PIV) technique. The flow was seeded with incense smoke and was illuminated by a Surelite LSI-10 (Continuum) Nd:YAG pulsed laser with a power of 170 mJ/pulse. The light sheet optics includes spherical and cylindrical Galilei telescopes with tuneable divergence and adjustable focus length. We used a progressive-scan 12 bit digital CCD camera (pixel size $6.7 \mu\text{m} \times 6.7 \mu\text{m}$ each) with a dual-frame-technique for cross-correlation processing of captured images. A programmable Timing Unit (PC interface card) generated sequences of pulses to control the laser, camera and data acquisition rate. The data was processed using standard cross correlation techniques (DaVis 7.0 code, LaVision, Göttingen).

An incense smoke with sub-micron particles as a tracer for the PIV measurements was produced by high temperature sublimation of solid incense particles. Analysis of smoke particles using a microscope (Nikon, Epiphot with an amplification of 560) and a PM-300 portable laser particulate analyzer showed that these particles have an approximately spherical shape and that their mean diameter is of the order of $0.7 \mu\text{m}$. In order to prevent from any thermal effects caused by the incense smoke generator, we placed it far away from the test section behind a wall, so that the incense smoke was transported through a five meter long pipeline and was cooled before it entered the test section. The smoke was feeded into the test section at room temperature. We measured the smoke temperature inside the pipeline at two locations: 0.5 m and 3.5 m from the generator. At the first location the smoke temperature was 318 K, while at the second location it was 294 K. The number density of smoke particles inserted to the test section in the experiments was of the order of 10^4 cm^{-3} .

We determined mean and r.m.s. velocities, two-point correlation functions and an integral scale of turbulence from the measured velocity fields. A series of 130 pairs of images acquired with a frequency of 4 Hz were stored for calculating the velocity maps and for ensemble and spatial averaging of turbulence characteristics. The center of the measurement region coincides with the center of the chamber. We measured the velocity in flow area of $92 \times 92 \text{ mm}^2$ with a spatial resolution of 1024×1024 pixels. These regions were analyzed with interrogation windows of 32×32 pixels. A velocity vector was determined in every interrogation window, allowing us to construct a velocity map comprising 32×32 vectors. The mean and r.m.s. velocities for each point of the velocity map (1024 points) were determined by averaging over 130 independent maps, and then over 1024 points. The

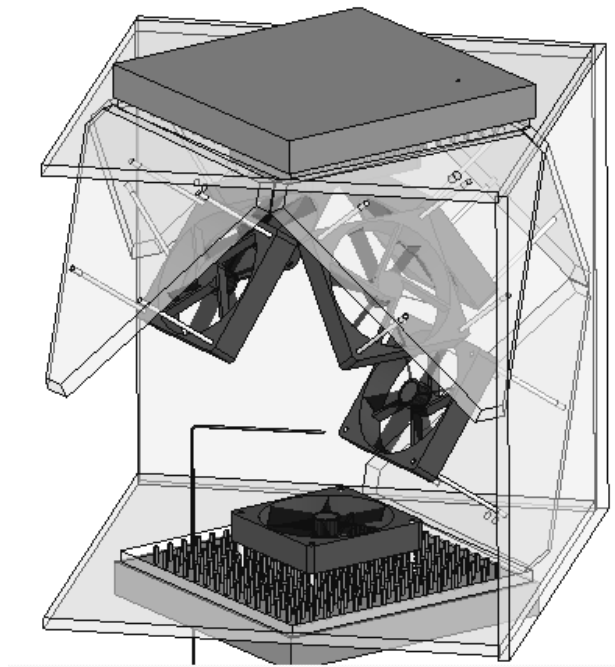


FIG. 2: The scheme of the temperature measurements. The wire that holds the thermocouple is inserted from the bottom of the chamber (some parts of the test section are not shown).

Table 1
Flow parameters in a multi-fan turbulence generator

Horizontal and vertical directions	Y	Z
Reynolds number $Re = uL/\nu$	703	875
Integral length scale L (mm)	14.85	16.4
r.m.s. velocity u (m/s)	0.71	0.8
Turbulence integral time scale $\tau = L/u$ (ms)	20.9	20.5
Rate of dissipation $\varepsilon = u^3/L$ (m^2/s^3)	24.1	31.2
Taylor microscale $\lambda = \sqrt{15\nu\tau}$ (mm)	2.17	2.15
Kolmogorov length scale $\eta = L Re^{-3/4}$ (μm)	109	102
$Re_\lambda = u\lambda/\nu$ in the Taylor microscale	103	115

two-point correlation functions of the velocity field were determined for each point of the central part of the velocity map (16×16 vectors) by averaging over 130 independent velocity maps, and then over 256 points. Our tests showed that 130 image pairs contain enough data to obtain reliable statistical estimates. An integral scale L of turbulence was determined from the two-point correlation functions of the velocity field. For this end we used exponential approximation of the correlation function since the experimentally measured correlation function did not reach zero values.

Spatial resolution of the velocity measurements was about 2.9 mm for a probed area $92 \times 92 \text{ mm}^2$ with interrogation window 32×32 pixels. The maximum tracer particle displacement in the experiment was of the order of 8 pixels, i.e., $1/4$ of the interrogation window. The average displacement of tracer particles was of the order of

2.5 pixels. Therefore, the average accuracy of the velocity measurements was of the order of 4% for the accuracy of the correlation peak detection in the interrogation window which was of the order of 0.1 pixels (see, e.g., Adrian 1991; Westerweel 1997; 2000).

In order to create large mean temperature gradient, the top and bottom fans were run at different speeds than the peripheral fans (see below). This regime was found empirically. Clearly, this introduces a weak anisotropy in velocity fluctuations in the vertical direction which is less than 10%. Note that the anisotropy of turbulence is not essential for the validation of the phenomenon of turbulent thermal diffusion.

Fluid flow parameters (at the rotation speed 1500 rpm for eight corner fans and 2300 rpm for top and bottom fans) at the horizontal Y and vertical Z directions are presented in Table 1. In the experiments the maximum mean flow velocity was of the order of 0.1–0.2 m/s while the r.m.s. velocity was of the order of 0.7–1.1 m/s. Thus, the measured r.m.s. velocity was much higher than the mean fluid velocity in the core of the flow. Figure 3 shows the two-point correlation functions of the velocity field at the horizontal and vertical directions. In particular, in Fig. 3 we plotted the longitudinal velocity correlation coefficients, $f(y) = \langle u_y(0)u_y(y) \rangle / \langle u_y^2(0) \rangle$ and $f(z) = \langle u_z(0)u_z(z) \rangle / \langle u_z^2(0) \rangle$, where \mathbf{u} are the fluid velocity fluctuations. Figure 3 and Table 1 demonstrate that the multi-fan turbulence generator produced a weakly anisotropic turbulent fluid flow with a small mean velocity.

The energy spectrum of the fluid flow is shown in Fig. 4. The one-dimensional longitudinal energy spectrum was determined by a standard procedure. In particular, we determined the Fourier components $u_y(k_y)$ and $u_z(k_z)$ of the fluctuating velocity field, and then determined $\langle |u_y(k_y)|^2 \rangle$ and $\langle |u_z(k_z)|^2 \rangle$, where $\langle \dots \rangle$ is the ensemble averaging over 130 independent velocity maps. In Fig. 4 we plotted horizontal and vertical energy component spectra. As can be seen from Fig. 4, the energy spectrum is different from $-5/3$ law. However, our study showed that the existence of the effect of turbulent thermal diffusion is independent of the slope of the energy spectrum.

Spatial particle number density distributions were obtained using a single frame from the double frame captured for PIV measurements. For this purpose the intensity of laser light Mie scattering by tracer particles was recorded and averaged over 130 single frames. We probed the central 9.2×9.2 cm region in the chamber by determining the mean intensity of scattered light in 32×16 interrogation windows with a size of 32×64 pixels. The vertical distribution of the intensity of the scattered light was determined in 16 vertical strips, which are composed of 32 interrogation windows. Variations of the obtained vertical distributions between these strips were very small. We used spatial average across the strips and ensemble average over 130 images of the vertical distributions of the intensity of scattered light. The turbu-

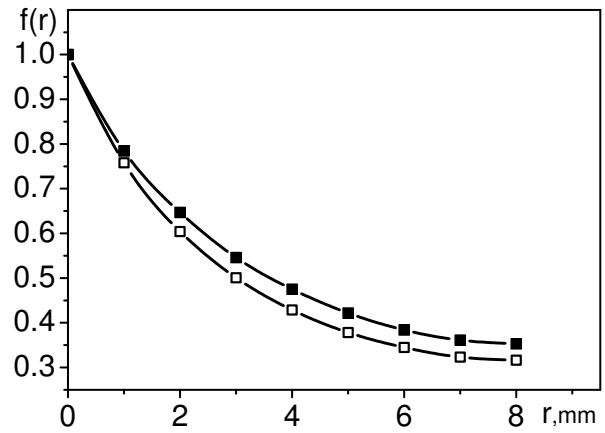


FIG. 3: The two-point longitudinal correlation functions of the velocity field at the horizontal direction (filled squares) and vertical direction (unfilled squares).

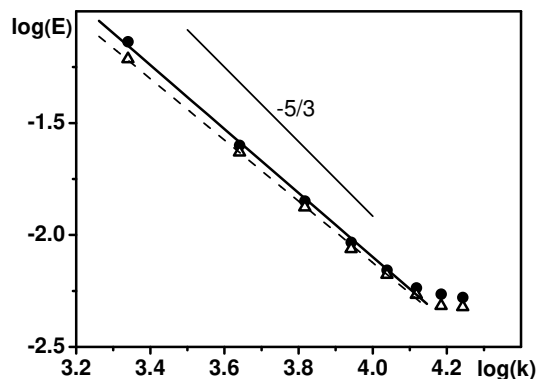


FIG. 4: The energy spectrum of the fluid flow.

lent diffusion coefficient in the test section D_T was of the order of $D_T \sim 40 \text{ cm}^2 / \text{s}$. The turbulent diffusion time $\tau_{TD} = L_d^2 / D_T \sim 3$ seconds in the scale of core flow $L_d = 10$ cm. Thus the steady state particle spatial distribution is reached during several seconds, while the turbulence integral time scale $\tau \sim 2 \times 10^{-2}$ s. The measurements were started several minutes after the seed was inserted in the chamber.

III. TURBULENT THERMAL DIFFUSION: THEORY AND EXPERIMENT

Now let us discuss the effect of turbulent thermal diffusion and compare the theoretical predictions with the experimental results. The mean number density of particles \bar{N} advected by a turbulent fluid flow is given by

$$\frac{\partial \bar{N}}{\partial t} + \text{div} [\bar{N}(\bar{\mathbf{V}} + \mathbf{V}_{\text{eff}}) - D_T \nabla \bar{N}] = 0, \quad (1)$$

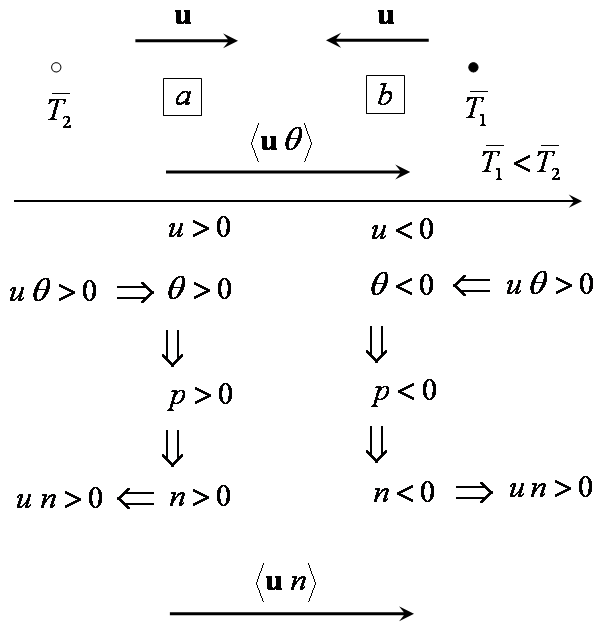


FIG. 5: Mechanism of turbulent thermal diffusion of inertial particles.

$$\mathbf{V}_{\text{eff}} = -\tau \langle \mathbf{u}_p \text{div} \mathbf{u}_p \rangle = -D_T (1 + \kappa) \frac{\nabla \bar{T}}{\bar{T}}, \quad (2)$$

where $D_T = (\tau/3)\langle \mathbf{u}^2 \rangle$ is the turbulent diffusion coefficient, τ is the momentum relaxation time of the turbulent velocity field, \mathbf{u} are fluctuations of fluid velocity, $\bar{\mathbf{V}}$ is the mean fluid velocity, \mathbf{u}_p are fluctuations of particle velocity, \bar{T} is the mean fluid temperature. Coefficient κ depends on particle inertia (the particle size a), the Reynolds number and the mean fluid temperature. In Eq. (1) we neglected a small molecular mean flux of particles caused by molecular (Brownian) diffusion, molecular thermal diffusion (or molecular thermophoresis) and small particle terminal fall velocity. Equation (1) was previously derived by different methods (see Elperin et al. 1996; 1997; 1998; 2000b; 2001; Pandya and Mashayek 2002; Reeks 2005).

For non-inertial particles, their velocity coincides with fluid velocity $\mathbf{v} = \bar{\mathbf{V}} + \mathbf{u}$, and $\text{div} \mathbf{v} \approx -(\mathbf{v} \cdot \nabla)\rho/\rho \approx (\mathbf{v} \cdot \nabla)T/T$, where ρ and T are the density and temperature of the fluid, and $\bar{\mathbf{V}} = \langle \mathbf{v} \rangle$. Therefore, the effective velocity of non-inertial particles $\mathbf{V}_{\text{eff}} = -\tau \langle \mathbf{u} \text{div} \mathbf{u} \rangle$ is given by $\mathbf{V}_{\text{eff}} = -D_T (\nabla \bar{T})/\bar{T}$. Here we used the equation of state for an ideal gas, and neglected small gradients of the mean fluid pressure. This effective velocity causes an additional turbulent flux of particles directed to the minimum of mean fluid temperature (phenomenon of turbulent thermal diffusion). Note that turbulent thermal diffusion for non-inertial particles is the purely kinematic effect. Indeed, the equation for the instantaneous mass concentration, $C = m_p n/\rho$, of non-inertial particles in

non-isothermal flow reads

$$\frac{\partial C}{\partial t} + (\mathbf{v} \cdot \nabla)C = \frac{1}{\rho} \text{div} (D \rho \nabla C), \quad (3)$$

where m_p is the particle mass and n is the instantaneous number density of particles. For very small molecular diffusion D , this equation reads

$$\frac{\partial C}{\partial t} + (\mathbf{v} \cdot \nabla)C \approx 0, \quad (4)$$

which implies that the mass concentration C is conserved along the fluid particle trajectory. In homogeneous turbulence all trajectories are similar. Therefore, the number density of non-inertial particles $n \propto \rho$, i.e., the number density of non-inertial particles behaves locally as the fluid density. In particular, the location of the maximum of the number density of non-inertial particles coincides with the location of the maximum of the fluid density, and vice versa. For very small mean fluid pressure gradients, $\nabla \bar{\rho}/\bar{\rho} \approx -\nabla \bar{T}/\bar{T}$, where $\bar{\rho}$ is the mean fluid temperature. Therefore, the location of the maximum of the mean number density of non-inertial particles coincides with the location of the minimum of the mean fluid temperature, and vice versa. The equation for the mean number density of non-inertial particles \bar{N} is equivalent to the following equation for the mean mass concentration $\bar{C} = m_p \bar{N}/\bar{\rho}$ of non-inertial particles:

$$\frac{\partial \bar{C}}{\partial t} + (\bar{\mathbf{V}} \cdot \nabla)\bar{C} = \frac{1}{\bar{\rho}} \text{div} (D_T \bar{\rho} \nabla \bar{C}). \quad (5)$$

If one ignores the turbulent thermal diffusion term in Eq. (1) for the mean number density of non-inertial particles \bar{N} , then the equation for the mean mass concentration \bar{C} of non-inertial particles has an incorrect form.

For inertial particles, their velocity \mathbf{v}_p depends on the velocity of the surrounding fluid \mathbf{v} . In particular, for a small Stokes time $\mathbf{v}_p \approx \mathbf{v} - \tau_p d\mathbf{v}/dt + O(\tau_p^2)$ (see Maxey 1987), where τ_p is the Stokes time. Using the Navier-Stokes equation it can be shown that $\text{div} \mathbf{v}_p \approx \text{div} \mathbf{v} + \tau_p \Delta P/\rho + O(\tau_p^2)$ (Elperin et al. 1996). The effective velocity (2) for inertial particles is given by $\mathbf{V}_{\text{eff}} = -D_T \alpha (\nabla \bar{T})/\bar{T}$, where the coefficient $\alpha = 1 + \kappa(a)$, $\kappa(a) \propto \tau_p \propto a^2$ and a is the particle size. Therefore, the mean particle velocity is $\bar{\mathbf{V}}_p = \bar{\mathbf{V}} + \mathbf{V}_{\text{eff}}$. Turbulent thermal diffusion implies an additional non-diffusive turbulent flux of inertial particles to the minimum of mean fluid temperature (i.e., the additional turbulent flux of inertial particles in the direction of the turbulent heat flux). In order to demonstrate that the directions of the turbulent flux of inertial particles and the turbulent heat flux coincide, let us assume that the mean temperature \bar{T}_2 at point 2 is larger than the mean temperature \bar{T}_1 at point 1 (see Fig. 5). Consider two small control volumes "a" and "b" located between these two points (see Fig. 5), and let the direction of the local turbulent velocity at the control volume "a" at some instant be the same as the direction of the turbulent heat flux $\langle \mathbf{u}\theta \rangle$ (i.e., it is

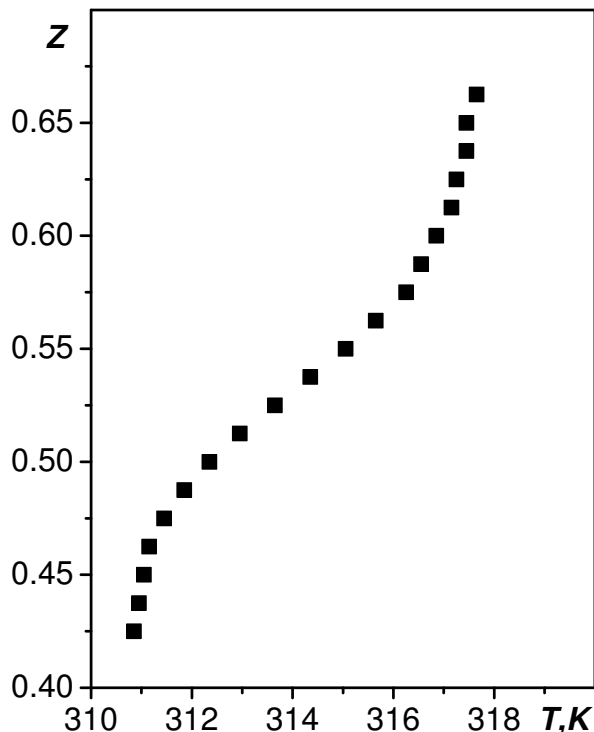


FIG. 6: Vertical temperature profile. Here Z is a dimensionless vertical coordinate measured in units of the height of the chamber, and $Z = 0$ at the bottom of the chamber.

directed to the point 1). Let the local turbulent velocity at the control volume "b" be directed at this instant opposite to the turbulent heat flux (i.e., it is directed to the point 2). In a fluid flow with an imposed mean temperature gradient, pressure p and velocity \mathbf{u} fluctuations are correlated, and regions with a higher level of pressure fluctuations have higher temperature and velocity fluctuations. Indeed, using equation of state of the ideal gas it can be easily shown that the fluctuations of the temperature θ and pressure p at the control volumes "a" are positive, and at the control volume "b" they are negative. Therefore, the fluctuations of the particle number density n are positive in the control volume "a" (because inertial particles are locally accumulated in the vicinity of the maximum of pressure fluctuations), and they are negative at the control volume "b" (because there is an outflow of inertial particles from regions with a low pressure). The mean flux of particles $\langle \mathbf{u}n \rangle$ is positive in the control volume "a" (i.e., it is directed to the point 1), and it is also positive at the control volume "b" (because both fluctuations of velocity and number density of particles are negative at the control volume "b"). Therefore, the mean flux of inertial particles $\langle \mathbf{u}n \rangle$ is directed, as is the turbulent heat flux $\langle \mathbf{u}\theta \rangle$, towards the point 1.

The contribution of turbulent thermal diffusion to the turbulent flux of particles is given by

$$J_T^{TTD} = -D_T \alpha \frac{\nabla \bar{T}}{\bar{T}} \bar{N} = -D_T k_T \frac{\nabla \bar{T}}{\bar{T}}, \quad (6)$$

where $D_T k_T$ is the coefficient of turbulent thermal diffusion, $k_T = \alpha \bar{N} = (1 + \kappa) \bar{N}$ is the turbulent thermal diffusion ratio, and the coefficient $\alpha = k_T / \bar{N}$ is the specific turbulent thermal diffusion ratio.

Neglecting the term $\bar{N} \mathbf{V}_{\text{eff}}$ in Eq. (1) for the mean number density of particles, we arrive at simple diffusion equation: $\partial \bar{N} / \partial t = D_T \Delta \bar{N}$, where we neglected a small mean velocity $\bar{\mathbf{V}}$. The steady-state solution of this equation is $\bar{N} = \text{const}$, i.e., a uniform spatial distribution of particles. On the other hand, our measurements in both, the multi-fan turbulence generator and an oscillating grids turbulence generator (Buchholz et al. 2004; Eidelman et al. 2004) demonstrate that the solution $\bar{N} = \text{const}$ is valid only for an isothermal turbulent flow. Let us take into account the effect of turbulent thermal diffusion in Eq. (1). Then the steady-state solution of Eq. (1) reads: $\nabla \bar{N} / \bar{N} = -\alpha \nabla \bar{T} / \bar{T}$, which yields

$$\frac{\bar{N}}{\bar{N}_0} = 1 - \alpha \frac{\bar{T} - \bar{T}_0}{\bar{T}_0}, \quad (7)$$

where $\bar{N}_0 = \bar{N}(\bar{T} = \bar{T}_0)$ and \bar{T}_0 is the reference mean temperature.

Now let us discuss the measurements of mean temperature and particle spatial distribution in the multi-fan turbulence generator, and compare the experimental results with the theoretical predictions. The mean temperature vertical profile in the multi-fan turbulence generator is shown in Fig. 6. Here Z is a dimensionless vertical coordinate measured in the units of the height of the chamber, and $Z = 0$ at the bottom of the chamber.

Measurements performed using different concentrations of the incense smoke in the flow showed that the distribution of the scattered light intensity normalized by the average over the vertical coordinate light intensity, is independent of the mean particles number density in the isothermal flow. In order to characterize the spatial distribution of particle number density, $\bar{N} \propto E^T / E$, in a non-isothermal flow, the distribution of the scattered light intensity E for the isothermal case was used to normalize the scattered light intensity E^T obtained in a non-isothermal flow under the same conditions. The scattered light intensities E^T and E in each experiment were normalized by corresponding scattered light intensities averaged over the vertical coordinate. The ratio E^T / E of the normalized average distributions of the intensity of scattered light as a function of the normalized vertical coordinate Z is shown in Fig. 7. A typical normalized E^T / E image in YZ plane is shown in Fig. 8. Inspection of Figs. 7-8 demonstrates that particles are redistributed in a turbulent flow with a mean temperature gradient, e.g., they accumulate in regions with minimum mean temperature (in the lower part of the chamber).

In order to determine the specific turbulent thermal diffusion ratio, α , in Fig. 9 we plotted the normalized particle number density $N_z \equiv \bar{N} / \bar{N}_0$ versus the normalized temperature difference $T_z \equiv (\bar{T} - \bar{T}_0) / \bar{T}_0$, where \bar{T}_0 is the reference temperature and $\bar{N}_0 = \bar{N}(\bar{T} = \bar{T}_0)$. Figure 9 was plotted using the mean temperature vertical profile

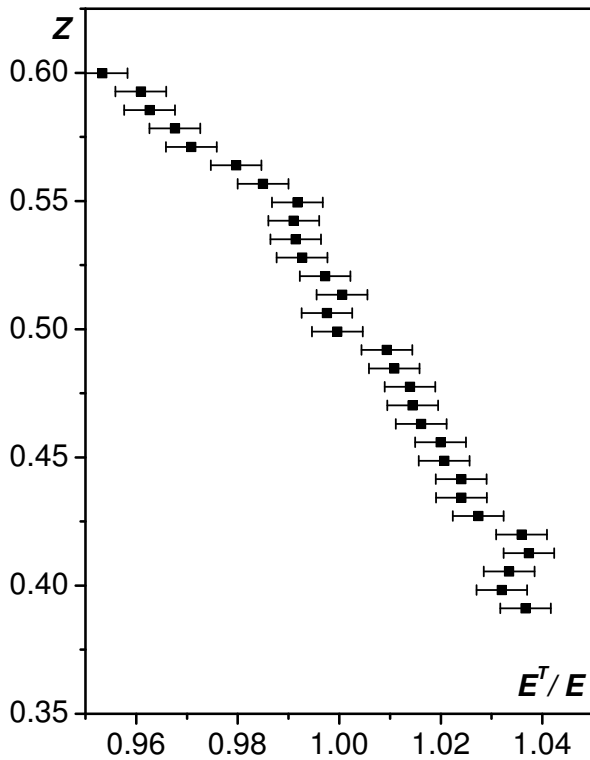


FIG. 7: Ratio E^T/E of the normalized average distributions of the intensity of scattered light versus the normalized vertical coordinate Z .

shown in Fig. 6. The normalized local mean temperatures [the relative temperature differences $(\bar{T} - \bar{T}_0)/\bar{T}_0$] in Fig. 9 correspond to the different locations inside the probed region. In particular, in Fig. 9 the location of the point with reference temperature \bar{T}_0 is $Z = 0$ (the lowest point of the probed region with a maximum \bar{N}). In these experiments we found that the coefficient $\alpha \approx 2.68$.

The specific turbulent thermal diffusion ratio α in the experiments with oscillating grids turbulence (Eidelman et al., 2004; Buchholz et al., 2004) was $\alpha = 1.29 - 1.87$ (depending on the frequency of the grid oscillations and on the direction of the imposed vertical mean temperature gradient), while in the multi-fan turbulence $\alpha = 2.68$. The latter value of the coefficient α is larger than that obtained in the experiments in oscillating grids turbulence, where the Reynolds numbers were smaller than those achieved in the multi-fan turbulence generator. Therefore, we demonstrated that the specific turbulent thermal diffusion ratio α increases with increase of Reynolds number. Note also that the experiments with oscillating grids turbulence were performed with two directions of the imposed vertical mean temperature gradient (for stable and unstable stratifications).

The specific turbulent thermal diffusion ratio, $\alpha = 1 + \kappa(a)$, comprises two terms, the first one (which equals to 1) is independent of the particle size and the second term depends on the size of particles. In particular,

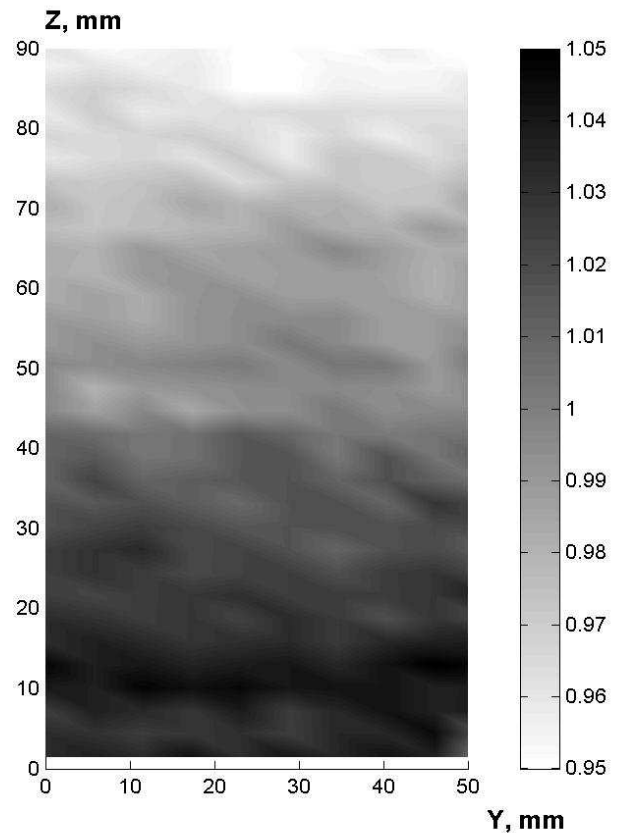


FIG. 8: A typical normalized E^T/E image in YZ plane. Here Y and Z are the horizontal and vertical coordinates.

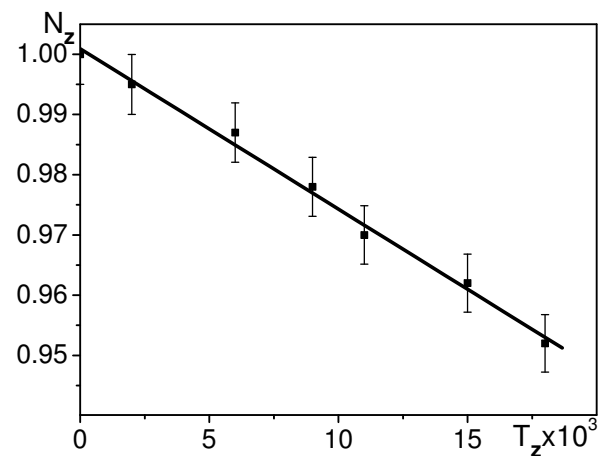


FIG. 9: Normalized particle number density $N_z \equiv \bar{N}/\bar{N}_0$ versus normalized temperature difference $T_z \equiv (\bar{T} - \bar{T}_0)/\bar{T}_0$.

$\kappa(a) \propto \tau_p \propto a^2$, where a is the particle size. For non-inertial particles, $\kappa(a) = 0$, and $\alpha = 1$. The deviation of the coefficient α in both experiments from $\alpha = 1$ is caused by a small yet finite inertia of the particles and also by the dependence of coefficient κ on the Reynolds numbers. The exact value of parameter α for inertial particles cannot be found within the framework of the theory

of turbulent thermal diffusion (Elperin et al. 1996; 1997; 1998; 2000b; 2001) for the conditions of our experiments (i.e., for large mean temperature gradients). However, in the experiments performed for different ranges of parameters and different directions of a mean temperature gradient, and in two different experimental set-ups, the coefficient α was more than 1, that agrees with the theory. Therefore, we demonstrated that turbulent thermal diffusion occurs independently of the method of turbulence generation.

The size of the probed region did not affect our results. The variability of the results obtained in different experiments was within 0.5%. This is caused by variability of optical conditions, light intensity variations in a light sheet and errors in light intensity detection. Therefore, it can be concluded that error in particle number density measurements is less than 0.5%. Note that the contribution of the mean flow to the spatial distribution of particles is negligibly small. In particular, the normalized distribution of the scattered light intensity measured in the different vertical strips in the regions where the mean flow velocity and the coefficient of turbulent diffusion may vary, are practically identical (the difference being only about 1%).

The effect of the gravitational settling of small particles ($0.5 - 1 \mu\text{m}$) is negligibly small (the terminal fall velocity of these particles being less than 0.01 cm/s). Due to the effect of turbulent thermal diffusion, particles are redistributed in the vertical direction in the chamber: particles accumulated in the lower part of the chamber, i.e., in regions with a minimum mean temperature. Some fraction of particles sticks to the fan propellers and chamber walls, and the total number of particles without feeding fresh smoke slowly decreases. The characteristic time of this decrease is about 15 minutes. However, the spatial distribution of the normalized number density of particles does not change over time. It must be noted that the accuracy of the measurements in these experiments ($\sim 0.5\%$) is considerably higher than the magnitude of the observed effect ($\sim 5\%$). Therefore, our experiments

detected the effect of turbulent thermal diffusion in the multi-fan turbulence generator. These results are in compliance with the results of the previous experiments in oscillating grids turbulence (see Buchholz et al. 2004; Eidelman et al. 2004).

IV. CONCLUSIONS

We studied experimentally the effect of turbulent thermal diffusion in a multi-fan turbulence generator using Particle Image Velocimetry and Image Processing Techniques. In a turbulent flow with an imposed vertical mean temperature gradient (stably stratified flow) particles accumulate in regions of minimum mean temperature. Therefore, our experiments detected the effect of turbulent thermal diffusion in the multi-fan turbulence generator, i.e., non-diffusive mean flux of particles in the direction of the mean heat flux. Turbulent thermal diffusion is an universal phenomenon. In particular, using two very different turbulent flows created by oscillating grids turbulence generator (Buchholz et al. 2004; Eidelman et al. 2004) and multi-fan turbulence generator, we demonstrated that the qualitative behavior of particle spatial distribution in non-isothermal turbulent flow is similar. The same physics is responsible for formation of particle inhomogeneities, i.e., competition between turbulent fluxes caused by turbulent thermal diffusion and turbulent diffusion.

Acknowledgments

We are grateful to two anonymous referees for their very helpful and important comments. This research was partly supported by the German-Israeli Project Cooperation (DIP) administered by the Federal Ministry of Education and Research (BMBF) and Israel Science Foundation governed by the Israeli Academy of Science.

-
- [1] Adrian RJ (1991) Particle imaging techniques for experimental fluid mechanics. *Ann. Rev. Fluid Mech.* 23: 261-304
 - [2] Aliseda A; Cartellier A; Hainaux F; Lasheras JC (2002) Effect of preferential concentration on the settling velocity of heavy particles in homogeneous isotropic turbulence. *J. Fluid Mech.* 468: 77-105
 - [3] Birouk M; Chauveau C; Sarh B; Quilgars A; Gokalp I (1996) Turbulence effects on the vaporization of mono-component single droplets. *Combustion Science and Technology* 413: 113-114
 - [4] Blackadar AK (1997) *Turbulence and diffusion in the atmosphere.* Springer, Berlin
 - [5] Buchholz J; Eidelman A; Elperin T; Grünefeld G; Kleeorin N; Krein A; Rogachevskii I (2004) Experimental study of turbulent thermal diffusion in oscillating grids turbulence. *Experiments in Fluids* 36: 879-887
 - [6] Csanady GT (1980) Turbulent diffusion in the environment. Reidel, Dordrecht
 - [7] Eaton JK; Fessler JR (1994) Preferential concentration of particles by turbulence. *Int J Multiphase Flow* 20: 169-209
 - [8] Eidelman A; Elperin T; Kleeorin N; Krein A; Rogachevskii I; Buchholz J; Grünefeld G (2004) Turbulent thermal diffusion of aerosols in geophysics and in laboratory experiments. *Nonlinear Processes in Geophysics* 11: 343-350
 - [9] Elperin T; Kleeorin N; Rogachevskii I (1996) Turbulent thermal diffusion of small inertial particles. *Phys Rev Lett.* 76: 224-228
 - [10] Elperin T; Kleeorin N; Rogachevskii I (1997) Turbulent barodiffusion, turbulent thermal diffusion and large-scale

- instability in gases. *Phys Rev E* 55: 2713-2721
- [11] Elperin T; Kleorin N; Rogachevskii I (1998) Formation of inhomogeneities in two-phase low-mach-number compressible turbulent flows. *Int J Multiphase Flow* 24: 1163-1182
- [12] Elperin T; Kleorin N; Rogachevskii I (2000a) Mechanisms of formation of aerosol and gaseous inhomogeneities in the turbulent atmosphere. *Atmosph Res* 53: 117-129
- [13] Elperin T; Kleorin N; Rogachevskii I; Sokoloff D (2000b) Turbulent transport of atmospheric aerosols and formation of large-scale structures. *Physics and Chemistry of the Earth A25*: 797-803
- [14] Elperin T; Kleorin N; Rogachevskii I; Sokoloff D (2001) Mean-field theory for a passive scalar advected by a turbulent velocity field with a random renewal time. *Phys Rev E* 64: 026304 (1-9)
- [15] Fallon T; Rogers CB (2002) Turbulence-induced preferential concentration of solid particles in microgravity conditions. *Experiments in Fluids* 33: 233-241
- [16] Fessler JR; Kulick JD; Eaton JK (1994) Preferential concentration of heavy particles in a turbulent channel flow. *Phys. Fluids* 6: 3742-3749
- [17] Flagan R; Seinfeld JH (1988) *Fundamentals of air pollution engineering*. Prentice Hall, Englewood Cliffs
- [18] Jaenicke R (1987) *Aerosol physics and chemistry*. Springer, Berlin
- [19] Korolev AV; Mazin IP (1993) Zones of increased and decreased concentration in stratiform clouds. *J. Appl. Meteorol.* 32: 760-773
- [20] Maxey MR (1987) The gravitational settling of aerosol particles in homogeneous turbulence and random flow field. *J Fluid Mech* 174: 441-465
- [21] Maxey MR; Chang EJ; Wang LP (1996) Interaction of particles and microbubbles with turbulence. *Experim. Thermal and Fluid Science* 12: 417-425
- [22] Pandya RVR; Mashayek F (2002) Turbulent thermal diffusion and barodiffusion of passive scalar and dispersed phase of particles in turbulent flows. *Phys Rev Lett* 88: 044501 (1-4)
- [23] Reeks MW (2005) On model equations for particle dispersion in inhomogeneous turbulence. *Int J Multiphase Flow* 31: 93-114
- [24] Seinfeld JH (1986) *Atmospheric chemistry and physics of air pollution*. John Wiley, New York
- [25] Shaw RA (2003) Particle-turbulence interactions in atmospheric clouds. *Ann. Rev. Fluid Mech.* 35: 183-227
- [26] Wang LP; Maxey MR (1993) Settling velocity and concentration distribution of heavy particles in homogeneous isotropic turbulence. *J. Fluid Mech.* 256: 27-68
- [27] Westerweel J (1997) *Fundamentals of digital particle image velocimetry*. *Meas. Sci. Technology* 8: 1379-1392
- [28] Westerweel J (2000) Theoretical analysis of the measurement precision of particle image velocimetry. *Exp. Fluids, Suppl.* 29: S3-S12